Available online at www.sciencedirect.com
SCIENCE DIRECT®
Polymer 45 (2004) 3827–3834
polymer
www.elsevier.com/locate/polymer

An explanation of silicate exfoliation in polyacrylonitrile/silicate nanocomposites prepared by in situ polymerization using an initiator adsorbed on silicate

Yeong Suk Choi, In Jae Chung*

Department of Chemical and Biomolecular Engineering, Korea Advanced Institute of Science and Technology (KAIST), 373-1 Guseong-dong, Yuseong-gu, Daejeon 305-701, South Korea

Received 29 September 2003; received in revised form 1 March 2004; accepted 12 March 2004

Abstract

Sodium montmorillonite (Na-MMT) absorbed a radical initiator, potassium persulfate (KPS), by way of hydrogen bonding between hydroxyl groups in the Na-MMT lattice and the sulfonic anions of KPS. FT-IR absorbance bands of hydroxyl groups in the Na-MMT lattice and the sulfonic anions of KPS shifted to lower wavenumber regions, compared with the free silicate and the initiator. The amounts of initiator adsorbed on the silicate were determined by using thermogravimetric analysis. The initiator adsorbed on silicate (IAS) commenced the polymerization of acrylonitrile (AN), delaminating silicate layers in polyacrylonitrile (PAN)/silicate nanocomposites. Molecular weights of PANs extracted from the nanocomposites decreased as the amount of initiator in IAS increased. Heterogeneous nucleation, polymerization in the basal spacing of the silicate layers, was analyzed by high performance liquid chromatograph. Storage moduli, E', of the nanocomposites were enhanced with the molecular weights of PAN matrixes. Glass temperatures, T_g, of the nanocomposites were dependent on the molecular weights of the PAN matrixes and the contents of the 2-acrylamido-2-methyl-1-propanesulfonic acid (AMPS) charged.

Keywords: Heterogeneous nucleation; Silicate; Nanocomposite

1. Introduction

Pinnavaia elucidated several properties of smectite clays in science [1]. Clays or phyllosilicates (abbreviated as 'silicate') have the properties of cation exchange, intercalation of molecules, and swelling in solvents. Their swelling capacity as a cation exchanger is fundamental to their intercalation and swelling properties. Swollen smectite clays can imbibe metal ions or neutral molecules. For example, when sodium montmorillonite (Na-MMT), one of the smectite clays, is immersed in a hydrophilic solvent such as water, the solvent expands the interlayer spaces of the silicate. Small molecules can penetrate into the interlayer spaces of clays [1,17] to form organic/inorganic hybrids, such as a silicate-supported initiator [7–16]. A silicate-supported initiator provides a useful way for the synthesis of polymer/silicate nanocomposites [2,3]. Giannelis et al. successfully intercalated an initiator into silicate, anchoring a free radical initiator in the gallery of silicate and synthesizing a polymer/silicate nanocomposite [4,5]. Another example for a catalyst using a silicate can be found in the living anionic polymerization of styrene initiated from silicate surfaces. Zhou et al. [9] used a 1,1-diphenylethylene derivative (DPE) as an initiator precursor. The DPE modified with a triethylammonium bromide was immobilized on the surface of silicate layers, and *n*-butyllithium (*n*-BuLi) was combined with the ethylene of DPE. Styrene was polymerized with the modified DPE.

In this paper, we prepared initiator adsorbed on silicate and synthesized polymer/silicate nanocomposites. This paper will explain several points that need discussion on the properties of polymer/silicate nanocomposites, and it will offer a new, simple method to exfoliate silicate layers in a polymer/silicate nanocomposite. Firstly, various amounts of a conventional radical initiator, KPS, will be adsorbed on silicate layers. Secondly, a series of polyacrylonitrile (PAN)/silicate nanocomposites, containing various molecular weights of PAN matrix and a fixed weight of the silicate

* Corresponding author. Tel.: +82-42-869-3916; fax: +82-42-869-3910.
E-mail address: chung@kaist.ac.kr (I.J. Chung).

0032-3861/$ - see front matter © 2004 Elsevier Ltd. All rights reserved.
doi:10.1016/j.polymer.2004.03.040

loaded [27–36], will be synthesized by using initiators adsorbed on silicate. The effect of molecular weight on the storage modulus of delaminated polymer/silicate nanocomposite has not been clearly explained yet, because the exfoliated morphology in the nanocomposite is not easily obtainable [18,24–26]. Thirdly, the variation of reactive surfactant amounts will alter the molecular weights of the PAN matrix, including their distributions, and that will explain the dependence of glass transition temperature, T_g, on the low molecular weight molecules in nanocomposites. Fourthly, the initiator adsorbed on the silicate will reveal the initiation mechanism in the polymerization [17]. Emulsion polymerizations [6] are generally initiated by initiator radicals and carried out, ideally, in one of two ways: homogeneous nucleation and heterogeneous nucleation. The former method involves the initiation of polymerization in a water phase by radicals from water-soluble initiators, and the latter method involves the commencement of polymerization inside monomer-swollen micelles by radicals transferred from a water phase into micelles. We illustrated that sodium montmorillonite (Na-MMT) is swollen by monomer. Therefore, we consider the silicate, when it was swollen by monomers and surfactants, as a monomer-absorbing receptacle, like a surfactant micelle, a heterogeneous phase, in an emulsion polymerization [17,18]. If a free-radical initiator solution is added to the aqueous silicate dispersion, polymerization can be carried out in one of two ways: a heterogonous nucleation within the galleries of silicate layers, containing a monomer, a surfactant, and water; or a homogeneous nucleation outside the silicate particles [19–23]. We restrict the presence of the initiator to the surface of the silicate layers, and this explains how the polymerization in the interlayer spaces of silicate, the heterogeneous nucleation, is carried out. The background for the selection of PAN as a polymer matrix is that acrylonitrile (monomer) is not a good solvent for its own polymer, so even though polymerization in the aqueous phase would take place, it would be difficult for the rigid PAN polymer chains to penetrate into the layer spaces of the silicate. Under these conditions, the expansion of silicate interlayer spaces by a polymer synthesized outside the silicate particles can be avoided.

2. Experimental section

2.1. Materials

Acrylonitrile and 2-acrylamido-2-methyl-1-propanesulfonic acid (AMPS) [37–39] were purchased from Aldrich and used as received. Sodium montmorillonite (Na-MMT) used in this experiment was Kunipia-F from Kunimine Co. and had 119 mequiv./100 g of cation exchange capacity. Pristine Na-MMT was dispersed in deionized water for 24 h at an ambient temperature, before use. Potassium persulfate (KPS), a radical initiator purchased from Junsei Chemical Co., was recrystallized using deionized water. *N,N*-Dimethylformamide (DMF) of high performance liquid chromatograph (HPLC) solvent grade was used as received from Aldrich for polymer recovery in a reverse ion exchange. Methyl alcohol (MeOH) from Fluka, a non-solvent for PAN, was distilled at normal pressure. Lithium chloride (Junsei) was recrystallized with tetrahydrofuran (THF).

2.2. Preparation of initiator adsorbed on silicate (IAS)

IAS was prepared by the following method. Deionized water of 145 g was put into a 250 ml flask fitted with a cover and then sodium montmorillonite (Na-MMT) of 5 g was charged into the flask. The mixture was stirred at room temperature until the aggregation of silicate in the deionized water was not observed. Various amounts of potassium persulfate (100, 90, and 50% of cation exchange capacity for the silicate) were added to the mixture, which was stirred for additional 24 h. By centrifuging the mixtures at 15,000 rpm for 30 min, IASs were segregated from the water, and they were redispersed in 100 ml of deionized water to remove the initiator unadsorbed on the silicate. This procedure was repeated 3 times until the water from centrifugation was free of initiators. It was confirmed by measuring the conductivity of the centrifuged water. The silicate cakes were freeze-dried for 5 days, and then placed in a refrigerator to prevent thermal decomposition.

2.3. Synthesis of PAN/silicate nanocomposites using initiator adsorbed on silicate (IAS)

PAN/silicate nanocomposites were prepared using the IASs in the following method: 0.5 g of IAS and 100 g of deionized water were charged into a 1000 ml four-neck glass reactor fitted with a condenser, a rubber septum, a stirrer, and a nitrogen inlet; the mixture was then stirred at 200 rpm for 5 h, in a nitrogen atmosphere at room temperature, to disperse the silicate. 2-acrylamido-2-methyl-1-propanesulfonic acid (AMPS, 0.3 g), dissolved in acrylonitrile (AN, 10 g), was charged to the reactor through a glass syringe, and stirred for 30 min to make the mixture disperse uniformly. The reactor temperature was raised to 65 °C to initiate the polymerization, and this temperature was maintained for 5 h. After polymerization, PAN/silicate nanocomposite was recovered by way of a freeze-drying process.

2.4. Polymer recovery

A small part of the freeze-dried nanocomposite was extracted with DMF/LiCl solution (60 g/0.2 g = DMF/LiCl) under a nitrogen atmosphere at 80 °C for 5 days in a 500 ml three-neck reactor fitted with a condenser, a nitrogen inlet and outlet. The mixture was centrifuged at 10,000 rpm for 30 min to separate PAN from the silicate

cakes. The extract was filtered with a 0.45 μm membrane filter to remove silicates and unwanted particles, and then poured into MeOH (10–20-fold) to precipitate PAN. The precipitated PAN was filtered and dried in a high vacuum at 50 °C for 50 h. The precipitated PAN was used for measuring the molecular weight.

2.5. Measurements

Infrared spectra were recorded on a Bomem 102 FT-IR spectrometer with KBr pellets. A total of 40 scans taken at 4 cm^{-1} of resolution were averaged.

X-ray diffraction patterns were obtained by using a Rigaku X-ray generator (Cu Kα with $\lambda = 0.15406$ nm) at room temperature, with a scanning rate of 2°/min in the 2θ range of 1.5–10°. X-ray diffraction patterns for the nanocomposites were obtained, after the nanocomposites were molded into a disk shape under 3000 psi, while X-diffraction patterns for the IASs were obtained in powder states after having been freeze-dried. For the water dispersion of silicate, the scan rate of X-ray was lowered to 0.5°/min to get a better resolution. Silicate and initiator dispersions before and after centrifugation were poured on glasses.

Oligomers formed in the aqueous phase were measured by using HPLC (HP 1100 series) equipped with a diode array detector and a C-8 column at a room temperature. The carrier solvent for HPLC was composed of water (80 g) and methyl alcohol (20 g), and the flow rate of the carrier solvent was controlled at 0.8 cm^3/min. The column was calibrated with AMPS, AN, and a mixture of AMPS and AN. The eluent was detected at 250 nm of wavelength by a reflective index (RI) detector.

Number-average molecular weights were determined by using gel permeation chromatography (GPC). GPC analyses were performed at a flow rate of 2.0 ml/min using DMSO at 80 °C, using a Waters GPC system equipped with six styragel HR columns (two 500, two 10^3, one 10^4, one 10^5) and a Water 410 RI detector, after calibration with five polystyrene standards obtained from Polymer Laboratories.

Thermogravimetric analyses (TGA) were carried out with a Perkin–Elmer thermobalance from room temperature to 600 °C, with a rate of 10 °C/min under N_2 atmosphere. Before measurements were taken, the initiator (KPS) and the IASs were heated isothermally at 100 °C for 10 min to remove any residual waters on them.

Tan δ and storage modulus (E') were obtained by a Rheometric Scientific DMTA4, with a dual cantilever from 30 to 180 °C and with a heating rate of 5 °C/min under 0.04% of deformation at 1 Hz of frequency. Samples were molded to a size of $11 \times 28 \times 1$ mm^3 at 140 °C for 2 min under 3000 psi of pressure. The glass transition temperatures, T_g, were determined from the maximum values in tan δ vs. the temperature scans.

The morphology of the nanocomposite was examined by a Philips CM-20 transmission electron microscope (TEM). The nanocomposite was sliced to a thickness of 100 nm and coated with carbon. The accelerating voltage of TEM was 160 kV.

3. Results

In the name of the sample, N denotes acrylonitrile (AN), A stands for AMPS, T indicates Na-MMT, and the numbers following A and N indicate the weight of each component. The numbers next to T indicate the relative weight percentages of Na-MMT to the weight of AN. The numbers 1, 2, and 3, next to IAS indicate that the initiators were added to the silicate with molar ratios of 100, 90, and 50% of the cation exchange capacity (CEC) of the silicate.

The adsorption of the initiator on Na-MMT is described by using FT-IR spectroscopy. Fig. 1 shows the FT-IR spectra of (a) pristine silicate, (b) potassium persulfate (initiator, KPS), (c) initiator adsorbed on silicate before centrifugation, and (d) initiator adsorbed on silicate after centrifugation (IAS1). In Fig. 1(c), an absorbance band assigned to the O–H stretching in silicate lattices shifts to 3627 cm^{-1} from its original wavenumber at 3633 cm^{-1} [40], and an absorbance band assigned to the S=O stretching motion of KPS moves to lower wavenumber regions, to 1292–1267 from 1299–1276 cm^{-1}. An absorbance band due to S–O stretching of KPS in IAS1 also becomes broad at 723–692 cm^{-1} from its unadsorbed state at 692 cm^{-1}. A Na-MMT unit cell has four hydroxyl groups as expressed in the following formula: $M^{n+}_{x/n}{\cdot}yH_2O[Al_{4.0-x}Mg_x](Si_{8.0})O_{20}$-(OH)4, where $M^{n+}_{x/n}$ is a monovalent cation, a sodium cation in this case [1], and the surface charge of Na-MMT is neutralized by exchangeable cations, sodium cations, so that the sulfonic anions have the possibility of hydrogen bonding with O–H groups in the silicate lattice or adsorbed

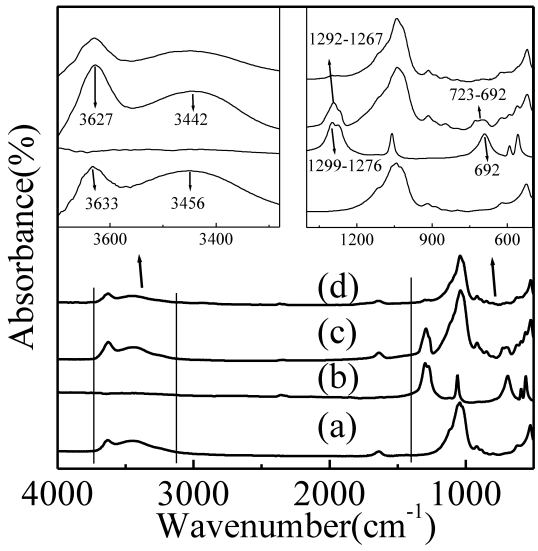

Fig. 1. FT-IR spectra of (a) pristine silicate, (b) potassium persulfate (KPS), (c) initiator adsorbed on silicate before centrifugation, (d) initiator adsorbed on silicate after centrifugation (IAS1).

water. Interaction between hydroxyl groups of silicate and sulfonic ions of KPS may cause the shifts of absorbance bands, and the absorbance band shifts indicate that the silicate may absorb the initiator through hydrogen bonding. After centrifugation in Fig. 1(d), the FT-IR spectrum of IAS1 has the weak characteristic absorbance bands at 1292 and 702–560 cm^{-1} corresponding to S=O and S–O stretching of the initiator. The absorbance bands at about 3627, 1040, 520, and 466 cm^{-1} are assigned to O–H stretching, Si–O stretching, Al–O stretching, and Si–O bending of the silicate in IAS1. These bands indicate the presence of the radical initiators on the surface of the silicate.

Fig. 2 shows X-ray diffraction patterns of the IASs and the pristine silicate. Before centrifugation, IAS1, IAS2, and IAS3 show traces of diffraction patterns of (001) planes at 7–8° in Fig. 2(a). The X-ray diffraction patterns indicate that the initiator and water enlarge the basal spacings of the silicate. After centrifugation of the dispersions, however, the diffraction patterns due to (001) planes of IAS1, IAS2, and IAS3 occur at about 7.55, 7.56, and 7.77° in Fig. 2(b), and their d_{001} spacings are 1.14, 1.170, and 1.172 nm, respectively. As the amount of initiator added to the silicate increases, the X-ray peak moves slightly toward a low angle. The differences in X-ray peak positions are so small that the silicate structures in IASs are not affected.

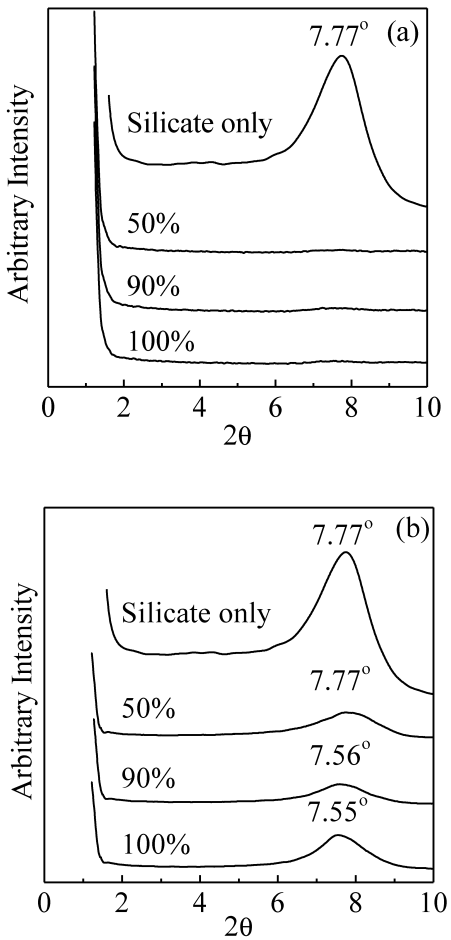

Fig. 2. X-ray diffraction patterns of initiator adsorbed on silicate (IAS) containing various amounts of initiators (KPS) and pristine silicate: (a) before centrifugation and (b) after centrifugation. 100, 90, and 50% indicate the molar ratio of charged initiator to the cation exchange capacity of unit weight of silicate.

The amount of an initiator loaded on a silicate is determined using the residual weight difference between IASs and the pristine silicate from thermogravimetric analysis (TGA) at 600 °C in Fig. 3. The residual weight percentage of pristine silicate at 600 °C is 98.52%, and those of IAS1, 2, 3 are 97.00, 97.78, and 98.21%, respectively. The residue of the initiator is 39.71% at 600 °C. The amount of the initiator in IAS is calculated by the residual difference between pristine silicate and IASs divided by 0.3971, the residue of the initiator. IAS1 contains 25.85 mg of KPS in 1 g of silicate. IAS2 has 12.25 mg of KPS and IAS3 has 5.13 mg of KPS. As we expected from the data of FT-IR and XRD, the amounts of KPS in the IASs are very small.

Fig. 4 shows FT-IR spectra of a pristine silicate, AMPS, and a PAN/silicate nanocomposite (A0.3N10T5%IAS2). The spectrum of A0.3N10T5%IAS2 in Fig. 4(c) exhibits characteristic absorbance bands of all the components. C–H stretching at 2939 cm^{-1}, C≡N stretching at 2243 cm^{-1}, and C–H bending at 1454 cm^{-1} are the characteristic absorbance bands of PAN. N–H bending at 1543 cm^{-1} and S=O stretching at 1369–1220 cm^{-1} are assigned to the vibration modes of AMPS. Absorbance bands from O–H stretching at 3624 cm^{-1}, Si–O stretching at 1041 cm^{-1}, Al–O stretching at 628 cm^{-1}, and Si–O bending at 522 cm^{-1} confirm the presence of the silicate in the nanocomposite.

Before the polymerization, we measure the d_{001} spacing of IAS2 dispersed in water by using X-ray diffraction with a scan rate of 0.5°/min. The d_{001} spacing provides a large

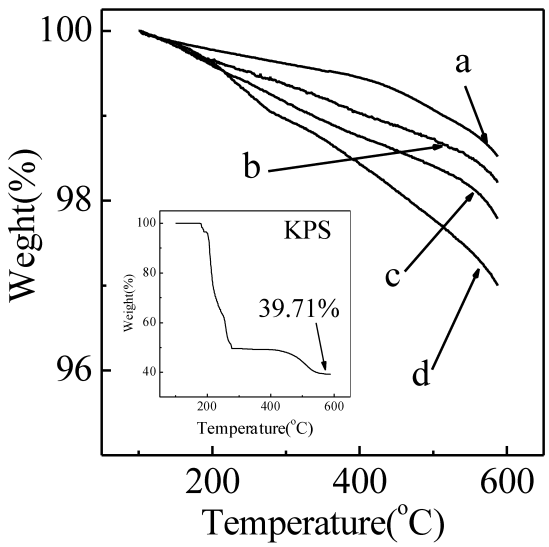

Fig. 3. Thermal gravimetric curves for initiator adsorbed on silicate (IAS), pristine silicate, and the initiator under a nitrogen atmosphere; (a) pristine silicate, (b) IAS3 containing 50% to CEC, (c) IAS2 containing 90% to CEC, and (d) IAS1 containing 100% of initiator to CEC value of silicate. KPS stands for the initiator, potassium persulfate.

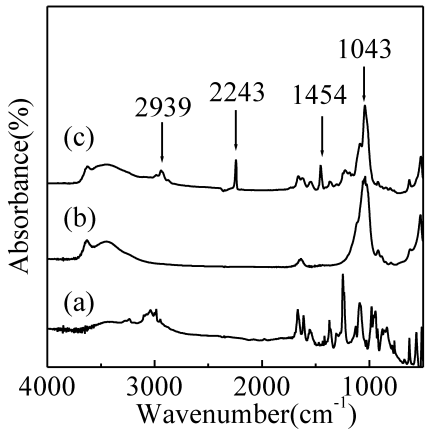

Fig. 4. FT-IR spectra of (a) reactive surfactant (AMPS), (b) pristine silicate, and (c) A0.3N10T5%IAS2.

amount of information regarding the exfoliation behavior of silicate layers and the reaction mechanism of monomer during polymerization. In Fig. 5(a), the diffraction pattern of the (001) plane of IAS2 dispersed in water reveals a weak and broad peak at 6.0° shifted by about 1.7° from its original position (7.77° in Fig. 2) and its d_{001} spacing is 1.47 nm. It means that water molecules enlarge the basal spacing of IAS2. When monomer (AN) is added to this IAS2 dispersion, the peak appears at 5.47° in Fig. 5(b), and d_{001} spacing is 1.62 nm. When only AMPS is added to the IAS2 dispersion, the peak in Fig. 5(c) is 5.25°, and d_{001} spacing is 1.68 nm. Finally, when both AN and AMPS are added to the IAS2 dispersion, the peak appears at 4.39° in Fig. 5(d), and d_{001} spacing is 2.01 nm. This expansion of d_{001} spacing will facilitate the polymerization in the galleries of IAS2. In our previous papers on PMMA [17] and PAN/silicate nanocomposites [18], silicate dispersed in water with monomers and AMPS was not observable. It can be inferred that the polymerization between interlayer spaces of silicate leads the nanocomposites to the exfoliated state. The expansion of

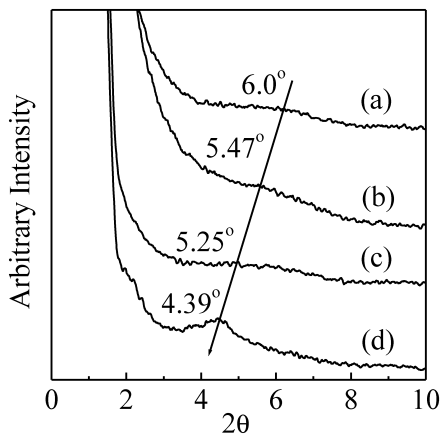

Fig. 5. X-ray diffraction patterns of the aqueous dispersions of IAS2 under various conditions: (a) the aqueous dispersion of IAS2, (b) the aqueous dispersion of IAS2 with acrylonitrile (AN), (c) the aqueous dispersion of IAS2 with the reactive surfactant (AMPS), and (d) the aqueous dispersion of IAS2 with AN and AMPS.

IASs basal spacing by AN and AMPS is the precondition for the heterogeneous nucleation. The presence of AN and AMPS with an initiator in the IAS2 indicates that the initial polymerization will be carried out in interlayer spaces of IAS2, which is similar to the heterogeneous nucleation in emulsion polymerization.

A non-negligible possibility exists of polymerization within the aqueous phase, that is, a homogeneous nucleation, if dimers or trimers of AN are detected in the aqueous phase. Therefore, we checked the formation of dimers or trimers in the aqueous phase using HPLC. The solution sampled at a fixed time was filtered with a 0.2 μm membrane filter, and then the filtrate was injected to the HPLC. In Fig. 6, AMPS and AN have retention times of 2 and 4 min, respectively. Dimers or trimers are not detected within the measurement range. This fact supports our previous interpretation of heterogeneous nucleation in Fig. 5.

Small parts of the nanocomposites were extracted with THF to remove oligomers or water molecules, which expand the basal spacings of the silicate. The extracted nanocomposites were dried under a high vacuum at 50 °C for 50 h and molded into a disk-like shape at 3000 psi of pressure. X-ray diffraction patterns of the extracted nanocomposites have no visible peak in the range of 1.2–10° as shown in Fig. 7. No peak explains the delamination of silicate layers in the nanocomposites, which results from the polymerization in the galleries of the silicate, that is, the heterogeneous nucleation. The exfoliation behaviors of IASs can be depicted in the following way. The intercalation of AN in IAS2 before polymerization is confirmed by the X-ray measurement in Fig. 5, and the loaded amounts of the initiators in the IASs are very low, as shown in Table 1. Polymerization in the aqueous phase may be negligible from HPLC data, so most monomers (AN) are polymerized in the basal spacing of IAS2. Even though the polymerization of AN occurs in the water, the polymer molecules have difficulty penetrating into the galleries of the silicate

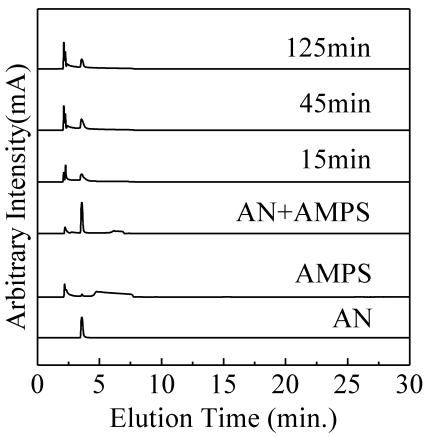

Fig. 6. HPLC chromatograms of the aqueous phases retrieved from A0.3N10T5%IAS1 during polymerization. AN, AMPS, and a mixture of AN and AMPS are given as standard materials.

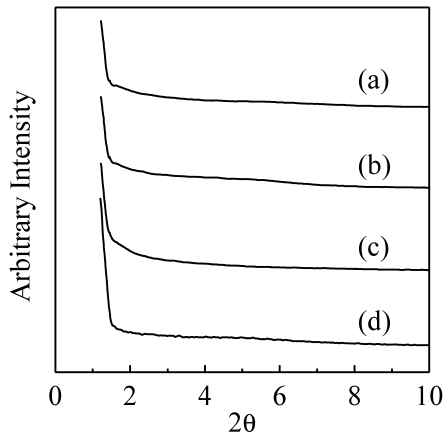

Fig. 7. X-ray diffraction patterns of the PAN/silicate nanocomposites of (a) A0.3N10T5%IAS1, (b) A0.3N10T5%IAS2, (c) A0.3N10T5%IAS3, and (d) A0.5N10T5%IAS1, extracted using THF for 12 h, using a Soxhlet extraction apparatus.

because of the rigidity of the PAN molecules (AN is a poor solvent to PAN). It may be concluded that the polymerization in the interlayer spaces of the silicate is the main cause for the exfoliation of the silicate. Table 1 shows the molecular weights of PANs extracted from the nanocomposites. Number-average molecular weights (M_n) of PAN decrease, as the contents of KPS in IASs increase. The reactive surfactant, AMPS, has some effect on molecular weights, because the nanocomposite with a high content of AMPS demonstrates a high value in M_n.

TEM is used to confirm the morphology of the PAN/silicate nanocomposite in Fig. 8, in which pristine silicate layers appear as dark strips, and PAN appears as white domains. The silicate layers in A0.3N10T5%IAS2 are well distributed and delaminated, so the exfoliated morphology of silicate is confirmed.

Now we consider the effect of molecular weights of PAN on the storage moduli of the nanocomposites. Storage moduli, E', of the nanocomposites in Fig. 9(a) increase with the molecular weights of the PAN. At 40 °C, storage moduli are 2.8×10^9 Pa for A0.3N10T5%IAS1, 3.99×10^9 Pa for A0.3N10T5%IAS2, and 4.34×10^9 Pa for A0.3N10T5%IAS3. A0.3N10T5%IAS2 demonstrates a 42% enhancement of storage modulus over A0.3N10T5%IAS1, and A0.3N10T5%IAS3 demonstrates

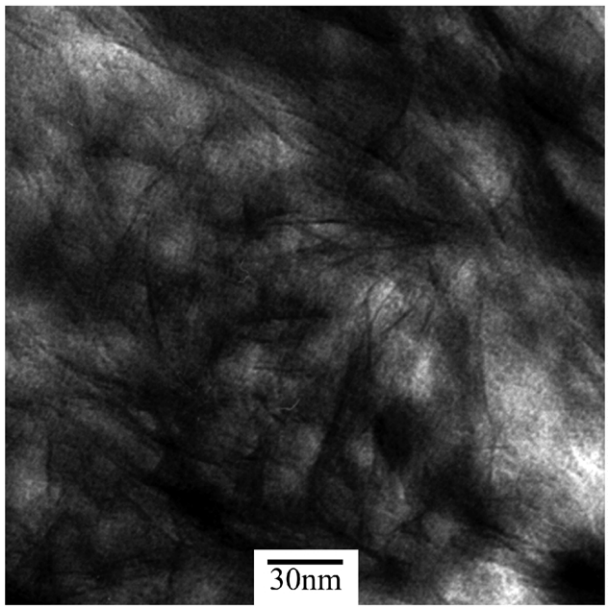

Fig. 8. TEM micrograph of A0.3N10T5%IAS2.

a 55% enhancement of storage modulus over A0.3N10T5%IAS1. Fig. 9(a) illustrates that the molecular weights of matrix polymers influence the storage moduli of the nanocomposites. In our other paper, we discussed how PAN/silicate nanocomposites [18] show an increase in modulus with an increase in the silicate contents. When the PAN/silicate nanocomposites containing 5 and 10 wt% of silicate loading were compared, the modulus enhancement by silicate was 45%. So the moduli of exfoliated nanocomposites can be enhanced by the molecular weights of polymers, as well as the contents of the silicate. In Fig. 9(b), we examine the effect of the reactive surfactant on the storage modulus of the nanocomposite. Compared with A0.3N10T5%IAS1, A0.5N10T5%IAS1 has a higher storage modulus in the low temperature range, but a lower modulus in the temperature range above 90 °C. The modulus decrease may be explained in the following way. Even though A0.5N10T5%IAS1 has a higher molecular weight, it has a wider molecular weight distribution of PAN (PDI = 2.99) than that of A0.3N10T5%IAS1. Therefore, it may contain molecules with lower molecular weights. Molecules with lower molecular weights tend to have high

Table 1
Molecular weights of polyacrylonitrile recovered from nanocomposites

Codes for clays	Molar ratio of initiator and CEC values of clay (%)	Amounts of initiator adsorbed on unit weight of silicate (mg)	
IAS1	100	25.85	
IAS2	90	12.25	
IAS3	50	5.13	
Codes for nanocomposites	M_n	M_w	PDI (M_w/M_n)
A0.3N10T5%IAS1	272,000	468,000	1.72
A0.5N10T5%IAS1	439,000	1,313,000	2.99
A0.3N10T5%IAS2	430,000	776,000	1.80
A0.3N10T5%IAS3	477,000	938,000	1.96

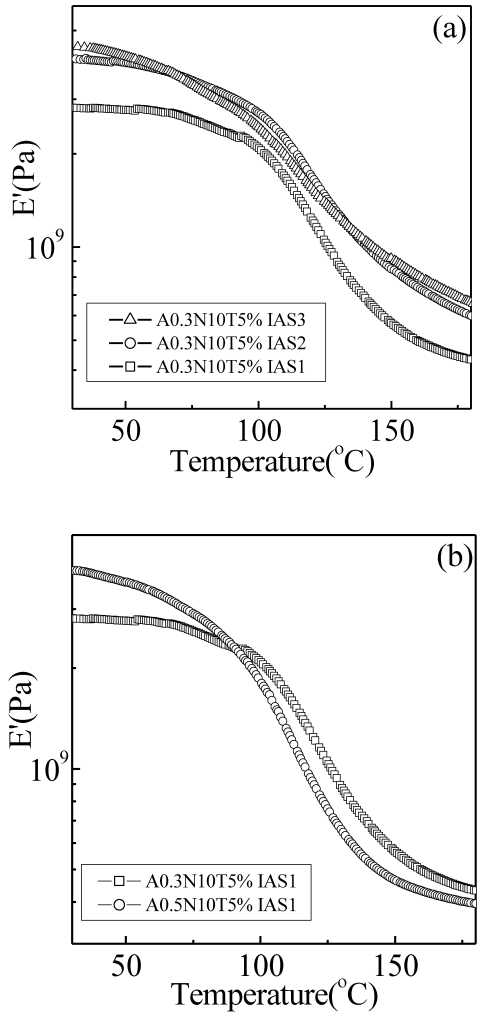

Fig. 9. Storage moduli of (a) PAN/silicate nanocomposites containing various molecular weights of PAN, and (b) PAN/silicate nanocomposites containing various AMPS contents measured by using DMA.

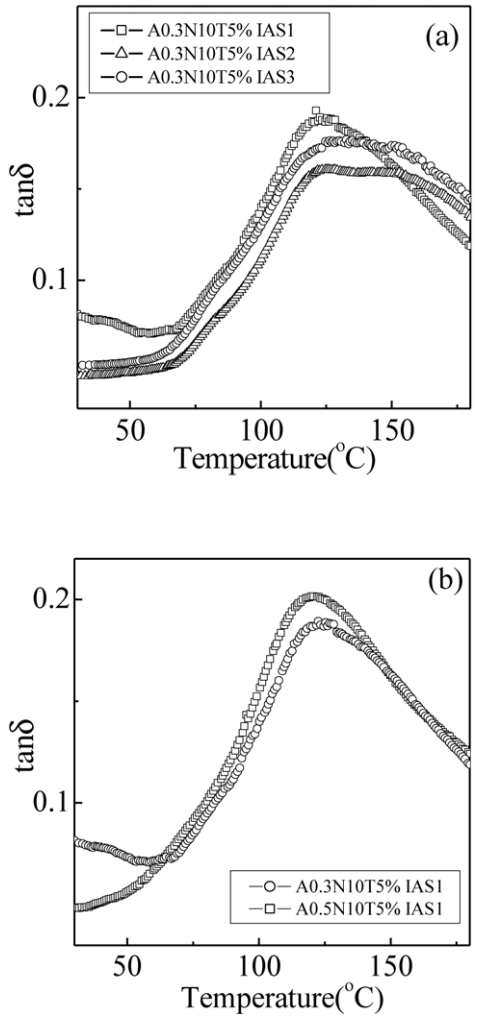

Fig. 10. tan δ of (a) PAN/silicate nanocomposites containing various molecular weights of PAN, and (b) PAN/silicate nanocomposites containing various AMPS obtained by using DMA.

molecular mobility at elevated temperatures, especially when the temperature approaches the polymer's glass transition temperature (T_g).

Glass transition temperatures (T_g) of the nanocomposites are obtained from the maximum peak temperatures of tan δ in Fig. 10. A0.3N10T5%IAS1, A0.3N10T5%IAS2, and A0.3N10T5%IAS3 have glass transition temperatures, T_g, at about 122, 123–151, and 126–149 °C, respectively. The glass transition temperatures, T_g, show an increasing correlation with the molecular weights of PAN. A0.3N10T5%IAS2 and A0.3N10T5%IAS3 have plateaus in tan δ scan. The polymers with high molecular weights in the nanocomposites are considered to slightly retard the segmental motion of the matrix and to increase the glass transition temperature. In Fig. 10(b), A0.5N10T5%IAS1 has a lower T_g at 120 °C than that of A0.3N10T5%IAS1, which has a T_g of 122 °C. The lower T_g may result from the higher portion of low molecular weights of PAN in A0.5N10T5%IAS1 than A0.3N10T5%IAS1.

4. Conclusion

Exfoliated PAN/silicate nanocomposites were prepared using initiators adsorbed on silicate. Adsorbed amounts of initiators on silicate were 25.85 mg for IAS1, 12.25 mg for IAS2, and 5.13 mg for In IAS3. The formation of dimmers or termers in the aqueous phase was not observed during polymerization, which suggested that the prime polymerization sites were in the galleries of IASs. The polymerization in the galleries of IASs demonstrated the heterogeneous nucleation. The molecular weights of PAN decreased with the amounts of initiator in the IASs. Storage moduli, E', of the nanocomposites were enhanced as the molecular weights of PAN increased, showing a 42% enhancement for A0.3N10T5%IAS2 and a 55% enhancement for A0.3N10T5%IAS3 over A0.3N10T5%IAS1. The glass transition temperature, T_g, of the nanocomposites increased with the increase of the molecular weights of PAN to 122, 123, and 126 °C for A0.3N10T5%IAS1,

A0.3N10T5%IAS2, and A0.3N10T5%IAS3, respectively. The contents of AMPS in composites depressed the glass transition temperature to 120, and 122 °C for A0.5N10T5%IAS1, and A0.3N10T5%IAS1, respectively. AMPS made the PDI of PAN broad, which indicated (1) that low molecules were included in the composites, and (2) that the low molecules affected the depressed glass transition temperatures.

Acknowledgements

The authors would like to express their sincere thanks to KOSEF (Korea Science and Engineering Foundation), to CAFPoly (Center for Advanced Functional Polymers), and to the BK 21 program for their financial support.

References

[1] Pinnavaia TJ. Science 1983;220:365.
[2] Usuki A, Kojima Y, Kawasumi M, Okada A, Fukushima Y, Kurauchi T, Kamigaito O. J Mater Res 1993;8:1179.
[3] Kojima Y, Usuki A, Kawasumi M, Okada A, Fukushima Y, Kurauchi T, Kamigaito O. J Mater Res 1993;8:1185.
[4] Weimer MW, Chen H, Giannelis EP, Sogah DY. J Am Chem Soc 1999;121:1615.
[5] Bergman JS, Chen H, Giannelis EP, Thomas MG, Coates GW. Chem Commun 1999;2179.
[6] Marestin C, Guyot A, Claverie J. Macromolecules 1998;31:1686.
[7] Hernando MJ, Pesquera C, Blanco C, González F. Chem Mater 2001; 13:2154.
[8] Yanagisawa M, Uchida S, Yin S, Sato T. Chem Mater 2001;13:174.
[9] Zhou Q, Fan X, Xia C, Mays J, Advincula R. Chem Mater 2001;13: 2465.
[10] Jordan R, West N, Ulman A, Chou YM, Nuyken O. Macromolecules 2001;334:1606.
[11] Templeton AC, Hostetler MJ, Kraft CT, Murray RW. J Am Chem Soc 1998;120:1906.
[12] Ejaz M, Yamamoto S, Ohno K, Tsujii Y, Fukuda T. Macromolecules 1998;31:5934.
[13] Kim DW, Blumstein A, Tripathy SK. Chem Mater 2001;13:1916.
[14] Karanikolopoulos G, Batis C, Pitsikalis M, Hadjichristidis N. Macromolecules 2001;34:4697.
[15] Gallis KW, Landry CC. Adv Mater 2001;13:23.
[16] Carrado KA, Xu L. Chem Mater 1998;10:1440.
[17] Choi YS, Choi MH, Wang KY, Kim SO, Kim YK, Chung IJ. Macromolecules 2001;34:8978.
[18] Choi YS, Wang KH, Xu M, Chung IJ. Chem Mater 2002;14:2939.
[19] Harkins WD. J Am Chem Soc 1947;69:1428.
[20] Smith WV, Ewart RH. J Chem Phys 1948;16:592.
[21] Sakota K, Okaya T. J Appl Polym Sci 1976;20:3265.
[22] Forcada J, Asúa JM. J Polym Sci Part A: Polym Chem 1990;28:987.
[23] Guo JS, Sudol ED, Vanderhoff JW, El-aasser MS. J Polym Sci Part A: Polym Chem 1992;30:691.
[24] Carrado KA, Xu L. Chem Mater 1998;10:1440.
[25] Bastow T, Hardin SG, Turney TW. J Mater Sci 1991;26:1443.
[26] Bergaya F, Kooli F, Alcover F. J Mater Sci 1992;27:2180.
[27] Svegliado G, Talamini G, Vidotto G. J Polym Sci Part A 1967;5:2875.
[28] Friedlander HN, Peebles LH, Brandup J, Kirby JR. Macromolecules 1968;1:79.
[29] Minagawa M, Iwamatsu T. J Polym Sci Polym Chem Ed 1980;18:481.
[30] Minagawa M, Miyano K, Takahashi M. Macromolecules 1988;21: 2387.
[31] Minagawa M, Takasu T, Shinozaki S. Polymer 1995;36:2343.
[32] Minagawa M, Onuma H, Ogita T, Uchida H. J Appl Polym Sci 2001; 79:473.
[33] Ko TH, Huang LC. J Appl Polym Sci 1998;70:2409.
[34] Thünemann A, Ruland W. Macromolecules 2000;33:2626.
[35] Thünemann A, Ruland W. Macromolecules 2000;33:1848.
[36] Viswanathan H, Wang YQ, Audi AA, Allen PJ, Sherwood PMA. Chem Mater 2001;13:1647.
[37] Seki M, Morishima Y, Kamachi M. Macromolecules 1992;25:6540.
[38] Morishima Y, Nomura S, Ikeda T, Seki M, Kamachi M. Macromolecules 1995;28:2874.
[39] Aota H, Akaki SI, Morishima Y, Kamachi M. Macromolecules 1997; 30:4090.
[40] Aranda P, Ruiz-Hitzky E. Appl Clay Sci 1999;15:119.